EUROPEAN ORGANIZATION FOR NUCLEAR RESEARCH

CERN-EP/88-25
February 29th, 1988

The Production of J/Ψ in 200 GeV/A Oxygen-Uranium Interactions.

M.C. Abreu [5], M. Alimi [6], C. Baglin [1], A. Baldit [3], G.P. Barreira [5], M. Bedjidian [6], P. Bordalo [5], S. Borenstein [4], J. Britz [8], A. Bussiere [1], P. Busson [4], A. Casaca [5], R. Cases [9], J. Castor [3], C. Charlot [4], B. Chaurand [4], D. Contardo [6], E. Descroix [6], A. Devaux [3], J. Fargeix [3], X. Felgeyrolles [3], P. Force [3], L. Fredj [3], J.M. Gago [5], C. Gerschel [7], P. Gomes [5], P. Gorodetzky [8], J.Y. Grossiord [6], A. Guichard [6], J.P. Guillaud [1], R. Haroutunian [6], L. Kluberg [4], L. Kraus [8], G. Landaud [3], I. Linck [8], C. Lourenço [5], A. Maio [5], L. Peralta [5], M. Pimenta [5], J.R. Pizzi [6], C. Racca [8], S. Ramos [5], A. Romana [4], R. Salmeron [4], A. Sinquin [7], P. Sonderegger [2] and J. Varela [5]

Abstract

The dimuon production in 200 GeV/nucleon oxygen-uranium interactions is studied by the NA38 Collaboration. The production of J/Ψ, correlated with the transverse energy E_T is investigated and compared to the continuum, as a function of the dimuon mass M and transverse momentum P_T. A value of 0.64 ± 0.06 is found for the ratio (Ψ/Continuum at high E_T)/(Ψ/Continuum at low E_T), from which the J/Ψ relative suppression can be extracted. This suppression is enhanced at low P_T.

Presented at Quark Matter 87
by
Andre Bussiere, LAPP, Annecy-le-Vieux, France.

---

1) LAPP, CNRS-IN2P3, Annecy-le-Vieux, France
2) CERN, Geneva, Switzerland
3) LPC, Univ. de Clermont-Ferrand and CNRS-IN2P3, France
4) LPNHE, Ecole Polytechnique and CNRS-IN2P3, Palaiseau, France
5) LIP, Lisbon, Portugal
6) IPNL, Univ. de Lyon and CNRS-IN2P3, Villeurbanne, France
7) IPN, Univ. de Paris-Sud and CNRS-IN2P3, Orsay, France
8) CRN ,CNRS-IN2P3 and Univ. Louis Pasteur, Strasbourg, France
9) IFIC, Burjasot, Valencia, Spain

1. INTRODUCTION.

NA38 is a dedicated experiment for the study of muon pairs produced in interactions of ultra-relativistic ions with dense matter. Several authors [1] have underlined the possibility that a phase transition could occur in such interactions, provided that the energy density reached is high enough. It would lead to a new state of matter, the quark-gluon plasma (quagma), which would exhibit specific observable properties.
Among the proposed signatures of the quagma, the production of lepton pairs has been advocated as one of the most direct [2], since it is not affected by the hadronization phase. More recently the suppression of the J/Ψ resonance has been predicted [3] and should provide a very clean signature. Moreover, this effect is expected to depend on the momentum of the dimuon [4]: the suppression should increase with decreasing momentum.
The results presented here are based on data taken with a 200 GeV/nucleon oxygen beam impinging on an uranium target. Muon pairs characteristics have been measured and correlated with the corresponding transverse energy produced in the collision.
The study of the data is still in progress and the results presented here reflect the status of the analysis at the time of the conference.

2. THE EXPERIMENT.

The experiment was run at very high intensities $(5-10)*10^7$ ions/burst, requiring very fast electronics and an efficient pile-up rejection. The apparatus was triggered on muon-pairs at a rate of $500-1000$ events per burst; a second level trigger, based on a CAB-microprocessor, rejected very low mass muon pairs, so that 250 events per burst could be recorded on tape with an acquisition livetime higher than 90 %. The apparatus consists of a muon spectrometer, an electromagnetic calorimeter, a multiple active target and specific beam detectors [5].

2.1 The spectrometer.

Fig.1 shows the lay-out of the spectrometer, already used at CERN in the NA10 experiment [6]. The muons produced at the target T are detected by two sets of four multiwire proportional chambers, CP1 – CP4 and CP5 – CP8, located respectively upstream and downstream of a magnet. Four hodoscopes, R1 – R4, made of plastic scintillators, provide the trigger. The magnet is an air-core toroid with hexagonal symmetry, which determines the geometrical structure of all the other components of the apparatus. A 4.8 m long absorber, located after the target, is used as a muon filter and allows also to dump the non-interacting part of the incident beam. Dimuons of mass larger than 0.5 GeV/c^2 are detected in the pseudo-rapidity range $2.8 < \eta < 4$ in the laboratory. For the J/Ψ, the mass resolution is 5 % and the acceptance 7 %.

2.2 The electromagnetic calorimeter.

The 12 cm long compact calorimeter has an outer radius of 12 cm and a central hole of 2.5 cm in diameter. It is made of scintillating fibers (1 mm diameter) embedded in lead in a $^1/_2$ volume ratio (X_0 = 8.3 mm). It is segmented in 30 cells, in a five rings arrangement covering the pseudo-rapidity range $2 < \eta < 4.2$ and exhibits the same hexagonal symmetry as the spectrometer. The energy resolution is $0.25/\sqrt{E}$.

2.3 The multiple active target.

Ten uranium subtargets (1 mm thick, 1x3 mm^2), 24 mm apart, are surrounded by 24 ring-scintillators, as shown in Fig.2. For each interaction, the energy deposited in each scintillator is measured, allowing the identification of the subtarget where the interaction took place, and the rejection of events with a secondary interaction.

2.4 The beam detectors.

As a consequence of the high intensity required by the experiment, pile-up rejection is mandatory in order to eliminate biased energy measurements. This is achieved by the use of two kind of detectors in the incident beam, as shown in Fig.2.
A beam hodoscope, made of two parallel planes of 14 and 16 scintillators respectively, is located 33 m upstream of the target, at a place where the beam spot is large enough to allow individual identification of the incoming ions. An efficient pile-up rejection is obtained by flagging events with more than one incident ion within the 20 ns gate of the ADC's.
Upstream and downstream of the active target, Fig.2, two quartz Cerenkov counters, immune to the high radiation level, are used for pile-up rejection, in conjunction with the beam-hodoscope. Their azimuthal segmentation in four quadrants allows a precise centering of the beam on the very small sub-targets.
Three sets of scintillator-telescopes, perpendicular to the beam-line, located around the target, are used to monitor the interaction rate.

3. DATA REDUCTION.

Data were taken in the fall of 1986 with a first period of 200 GeV protons on uranium. This was followed by an oxygen ion period at 200 GeV/nucleon and 60 GeV/nucleon, during which data were taken for oxygen-uranium and oxygen-copper interactions. Table 1 summarizes the characteristics of the beams and the number of reconstructed muon pairs for the various running conditions. The present analysis is based on a total of $2.5*10^6$ reconstructed muon pairs of any sign produced in oxygen-uranium collisions at 200 GeV/nucleon.
The data reduction, for the subsample of events taken at $5*10^7$ ion/burst, gives 450 K opposite-sign and 320 K like-sign pairs, after applying the following criteria, which reject 62 % of the events:

Pile-up (42 %) : only one incident ion.
Target (17 %) : one subtarget identified and no secondary interaction.
Trigger and Vertex (3 %): trigger conditions satisfied and calculated z-vertex in the target.

The sample of like-sign muon pairs is dominated by muons originating from π and K decays. It is used to determine the number of background events in the sample of opposite-sign pairs. The prompt dimuon signal is then given by the well known formula:

$$\text{signal} = (\mu^+\mu^-) - 2\sqrt{(\mu^+\mu^+)*(\mu^-\mu^-)}$$

Fig.3 shows the mass spectra for the opposite-sign and like-sign muon-pairs, and for the prompt dimuon signal. One should notice that the background is large in the raw spectra for low mass events, but is very small in the J/Ψ region. On the final mass spectrum, the J/Ψ resonance shows-up clearly above a steeply decreasing continuum originating mainly from Drell-Yan pairs and charmed particles decays.
The corresponding distributions of transverse neutral energy E_T are shown on Fig.4, for the opposite-sign, the like-sign pairs and for the signal. The shape of the distribution shows a depression in the low energy region, because our trigger favours collisions with a large number of participant nucleons. The measured transverse energy corresponds to about one half of the total transverse energy (neutral energy plus one third of the charged hadronic energy) in the covered pseudo-rapidity range. It should be noted that the values quoted for the transverse energy are "raw values" uncorrected for acceptance and smearing. The measured transverse energy will be used mainly as an indicator of the energy density of the interaction, because it is obviously correlated to the centrality of the collision.

4. ANALYSIS AND RESULTS.

The analysis presented here is a preliminary study of the J/Ψ production relative to the continuum, as a function of the transverse energy liberated in the collision. The predicted J/Ψ suppression would im-

crease of the relative yield of the resonance with increasing energy density which, in our experiment, is estimated from the neutral transverse energy E_T. In order to get rid of the low energy resonance region (ρ, ω, ϕ), the analysis is limited to muon pairs of mass larger than 1.7 GeV/c^2, a region where we can fit the shape of the continuum with a simple formula. We are then left with about 15000 events, roughly one half in the J/Ψ mass region (2.7 < M < 3.5 GeV/c^2) and one half in the continuum (1.7 < M < 5.3 GeV/c^2).
The mass spectrum has been fitted with the superposition of an exponential multiplied by $1/M^3$ for the continuum and two gaussians for the resonances J/Ψ and Ψ′ according to the following expression :

$$\frac{dN}{dM} = N_c \left\{ \frac{e^{\frac{-M}{M_c}}}{C_c * M^3} + \frac{N_\psi}{N_c} \left[\frac{e^{\frac{-(M-M_\psi)^2}{2\sigma^2_\psi}}}{C_\psi} + \frac{N_{\psi'}}{N_\psi} \frac{e^{\frac{-(M-M_{\psi'})^2}{2\sigma^2_{\psi'}}}}{C_{\psi'}} \right] \right\}$$

where C_c, C_ψ and $C_{\psi'}$ are normalization factors, M_ψ, $M_{\psi'}$, σ_ψ and $\sigma_{\psi'}$ are the masses and widths of the resonances, M_c is related to the slope of the continuum, N_ψ/N_c is the ratio of the J/Ψ over the continuum and $N_{\psi'}/N_\psi$ is the ratio of the Ψ′ over the Ψ. In a check of the reconstruction procedure, the fitted mass of the J/Ψ is M = 3.102 ± 0.003 GeV/c^2, and its width σ = 0.155 ± 0.003 GeV/c^2 agrees with the calculated mass resolution of the spectrometer.
In the following, M_ψ, $M_{\psi'}$, σ_ψ and $\sigma_{\psi'}$ are fixed and the three fitted parameters are M_c, N_ψ/N_c and $N_{\psi'}/N_\psi$. This last ratio appears to be meaningless, because of the poor statistics on the Ψ′. In order to look for the predicted J/Ψ suppression with increasing E_T, we study the ratio S of the fitted number of J/Ψ events relative to the fitted number of events in the continuum, in the mass range 2.5 < M < 3.5 GeV/c^2. (footnote)[1]
Fig.5 shows the fitted mass spectra for the events with low transverse energy (E_T < 28 GeV) and for those with high transverse energy (E_T > 50 GeV). Table 2 a) displays the fitted value of the parameter M_c and the ratio S in four E_T bands, choosen to be roughly equally populated. It shows a net decrease of S with increasing E_T : the J/Ψ-suppression appears from the ratio of the values of S for the extreme E_T bands

$$(\text{S at high } E_T)/(\text{S at low } E_T) = 0.64 \pm 0.06$$

On the contrary, the parameter of the continuum M_c remains constant, within errors, as E_T increases. It should be noted that the S values presented here do not include any acceptance correction and depend on the mass interval adopted for their determination. However, the ratio of S values in different E_T intervals should be independent of such a correction and other systematic effects.
In order to look for a possible dependence of the J/Ψ suppression on the transverse momentum P_T of the dimuon, the data have been divided into low-P_T events (P_T < 1 GeV/c) and high-P_T events (P_T > 1 GeV/c). The above fitting procedure has been applied to both P_T samples. The results are shown on Fig.6 for P_T > 1 GeV/c, and Fig.7 for P_T < 1 GeV/c. The values of S for P_T < 1 GeV/c and P_T > 1 GeV/c are given in Table 2 b). The ratios (S at high E_T/S at low E_T) are 0.72 ± 0.11 for P_T > 1 GeV/c and 0.53 ± 0.08 for P_T < 1 GeV/c, showing that the J/Ψ suppression is enhanced for low P_T.

---

[1] At the presentation at the conference, the interval used for the determination of S was misquoted as 2.7 < M < 3.5 GeV/c^2.

The dependence of the J/Ψ suppression on the transverse momentum P_T has also been investigated by studying the P_T distribution of events in the mass range corresponding to the J/Ψ, $2.7 < M < 3.5$ GeV/c^2. In fact these distributions, though dominated by true J/Ψ events, are contaminated by a small amount of continuum (from 7 % at low-E_T to 11 % at high-E_T). These P_T distributions, displayed on Fig.8 for the low E_T and the high E_T bins, show a steeper shape for low E_T. The ratio of these two P_T distributions, $R_\psi = (\Psi \text{ high } E_T)/(\Psi \text{ low } E_T)$, is plotted on Fig.9, as a function of the P_T of the J/Ψ. The ratio increases with increasing P_T, indicating that the J/Ψ suppression is more pronounced at low P_T. A linear fit through the ratios leads to a slope of 0.31 ± 0.06.
The same study of the E_T dependence of the P_T distributions has been performed for the events in the continuum with mass larger than 1.6 GeV/c^2, excluding the J/Ψ region ($2.7 < M < 3.5$ GeV/c^2). Fig.10 shows the ratio $R_c = (\text{Cont high } E_T)/(\text{Cont low } E_T)$ which is clearly independent of P_T, reflecting the fact that the P_T distribution of the continuum does not depend on transverse energy.
Finally a comparison has been made with the proton-uranium data at 200 GeV. The ratio $R_\psi = (\Psi \text{ high } E_T)/(\Psi \text{ low } E_T)$ is plotted on Fig.11, for the J/Ψ region ($2.7 < M < 3.5$ GeV/c^2), as a function of P_T. The ratio is found to be independent of P_T, as in Fig.10 (the corresponding slopes are both compatible with zero).

5. CONCLUSION

The dimuon production in 200 GeV/nucleon oxygen-uranium interactions, studied by the NA38 collaboration, shows that :

i) The ratio Ψ/Continuum (our parameter S) decreases with increasing E_T.
ii) The J/Ψ relative suppression can be expressed as:

$$(\text{S at high } E_T)/(\text{S at low } E_T) = 0.64 \pm 0.06$$

iii) This J/Ψ suppression is enhanced at low P_T.

The fact that the P_T-distribution of the continuum does not depend on E_T is an indication for J/Ψ suppression rather than continuum enhancement.
Although this effect has been predicted as a signature of quagma formation, it is not excluded that collective or nuclear effects could explain, at least partly, our experimental results.

ACKNOWLEDGMENTS

We would like to thank all the experts of the accelerator divisions of CERN, GSI and LBL for their efforts which have resulted in the development and acceleration of ion beams at CERN. We are grateful to the EA group for their work on our beam line. We are also indebted to the technical staff of the different institutions of the Collaboration for their contribution to the dectectors design, construction and setting up.

References

[1] Quark matter 84, Helsinki, Ed. K. Kajantie (Springer−Verlag 1985).
[2] K. Kajantie et al., Phys. Rev. D34 (1986) 811.
[3] T. Matsui and H. Satz, Phys. Let. 178B (1986) 416.
[4] F. Karsch, and R. Petronzio CERN−TH−4699/87 (1987).
[5] NA38 collaboration, to be published in Nucl. Inst. Meth..
[6] L. Anderson et al.,Nucl. Inst. Meth. 223 (1984) 26.

Table 1: Beam characteristics and number of reconstructed muon-pairs for the 1986 data

Beam	Energy	Intensity	Events
p + U	200 GeV/A	$5*10^7$ Ion/Burst	$6*10^5$ $\mu\mu$
O + U	200	$5*10^7$	$2*10^6$
O + U	200	10^8	$5*10^5$
O + Cu	200	$5*10^7$	$8*10^5$
O + U	60	$5*10^7$	$6*10^5$

Table 2: Fitted values of the continuum parameter M_c and the ratio $S = N_\psi/N_c$ in the range $2.5 < M < 3.5$ GeV/c²

	a) All P_T	
E_T	M_c	S
All E_T	1.21±.05	8.3±.3
$E_T < 28$ GeV	1.26±.1	9.3±.6
$28 < E_T < 40$	1.30±.1	7.9±.5
$40 < E_T < 50$	1.15±.1	7.4±.5
$E_T > 50$ GeV	1.35±.1	5.9±.4

	b) $P_T > 1.$ GeV/c		b) $P_T < 1.$ GeV/c	
E_T	M_c	S	M_c	S
All E_T	1.62±.1	10.9±.6	1.03±.05	6.8±.3
$E_T < 28$ GeV	1.83±.3	10.6±.9	1.01±.1	8.7±.8
$28 < E_T < 40$	1.77±.3	9.9±.9	1.07±.1	6.5±.6
$40 < E_T < 50$	1.58±.3	11.8±1.2	0.91±.1	5.7±.5
$E_T > 50$ GeV	1.37±.3	7.6±.8	1.33±.2	4.6±.5

FIGURE CAPTIONS

Fig.1
Lay-out of the dimuon spectrometer.

Fig.2
Lay-out of the electromagnetic calorimeter, the multiple active target and the beam detectors.

Fig.3
The mass spectra for the opposite-sign and like-sign muon pairs (a) and for the dimuon signal (b).

Fig.4
The measured transverse energy distributions for the opposite-sign and like-sign (background) pairs, and for the signal. These distributions contain 5 % of events satisfying the additional trigger condition $E_T > 40$ GeV.

Fig.5
The fitted mass spectra for events with low transverse energy (a) and for events with high transverse energy (b).

Fig.6
Same as Fig.5 but for events with high transverse momentum. ($P_T > 1$ GeV/c).

Fig.7
Same as Fig.5 but for events with low transverse momentum. ($P_T < 1$ GeV/c).

Fig.8
The P_T distributions, in the J/Ψ mass range $2.7 < M < 3.5$ GeV/c^2, for events with low transverse energy (a) and for events with high transverse energy (b). The lines correspond to simple exponential fits through the data.

Fig.9
The ratio (Ψ high E_T/Ψ low E_T) as a function of P_T.

Fig.10
The ratio (C high E_T/C low E_T), for the continuum events with $M > 1.6$ GeV/c^2, excluding the J/Ψ region.

Fig.11
Same as Fig.9, but for proton-uranium data.

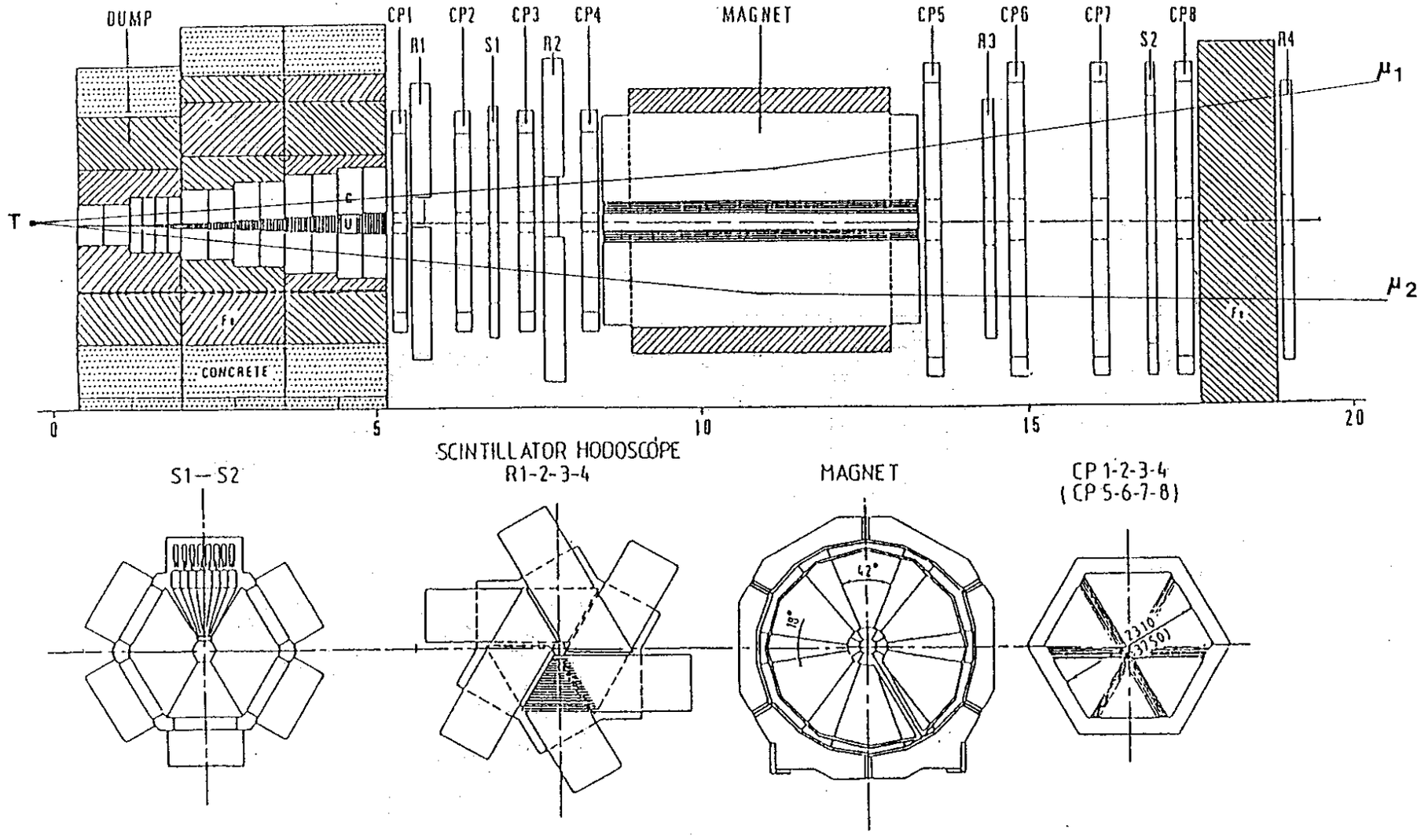
DUMP
CP1
CP2
CP3
CP4
MAGNET
CP5
CP6
CP7
CP8
R1
S1
R2
R3
S2
R4
T
μ_1
μ_2
C
U
Fe
CONCRETE
0
5
10
15
20
SCINTILLATOR HODOSCOPE
R1-2-3-4
S1—S2
MAGNET
CP 1-2-3-4
(CP 5-6-7-8)
42°
18°
23.10°
37.50°

Fig.1

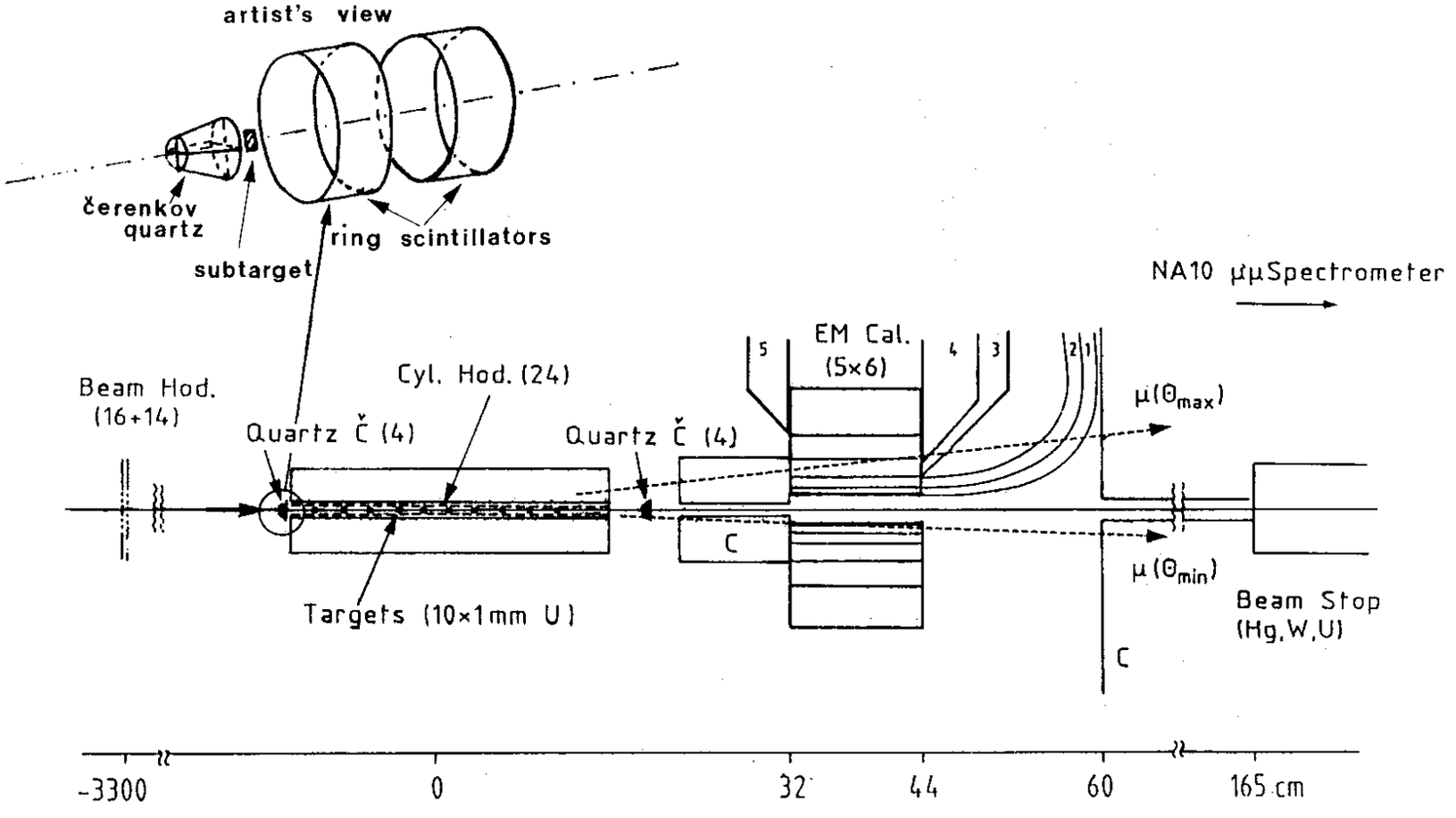
artist's view
čerenkov quartz
subtarget
ring scintillators
NA10 μμSpectrometer
EM Cal. (5×6)
5
4
3
2
1
Beam Hod. (16+14)
Cyl. Hod. (24)
Quartz Č (4)
Quartz Č (4)
μ(θmax)
C
μ(θmin)
Beam Stop (Hg,W,U)
Targets (10×1mm U)
C
-3300
0
32
44
60
165 cm

Fig.2

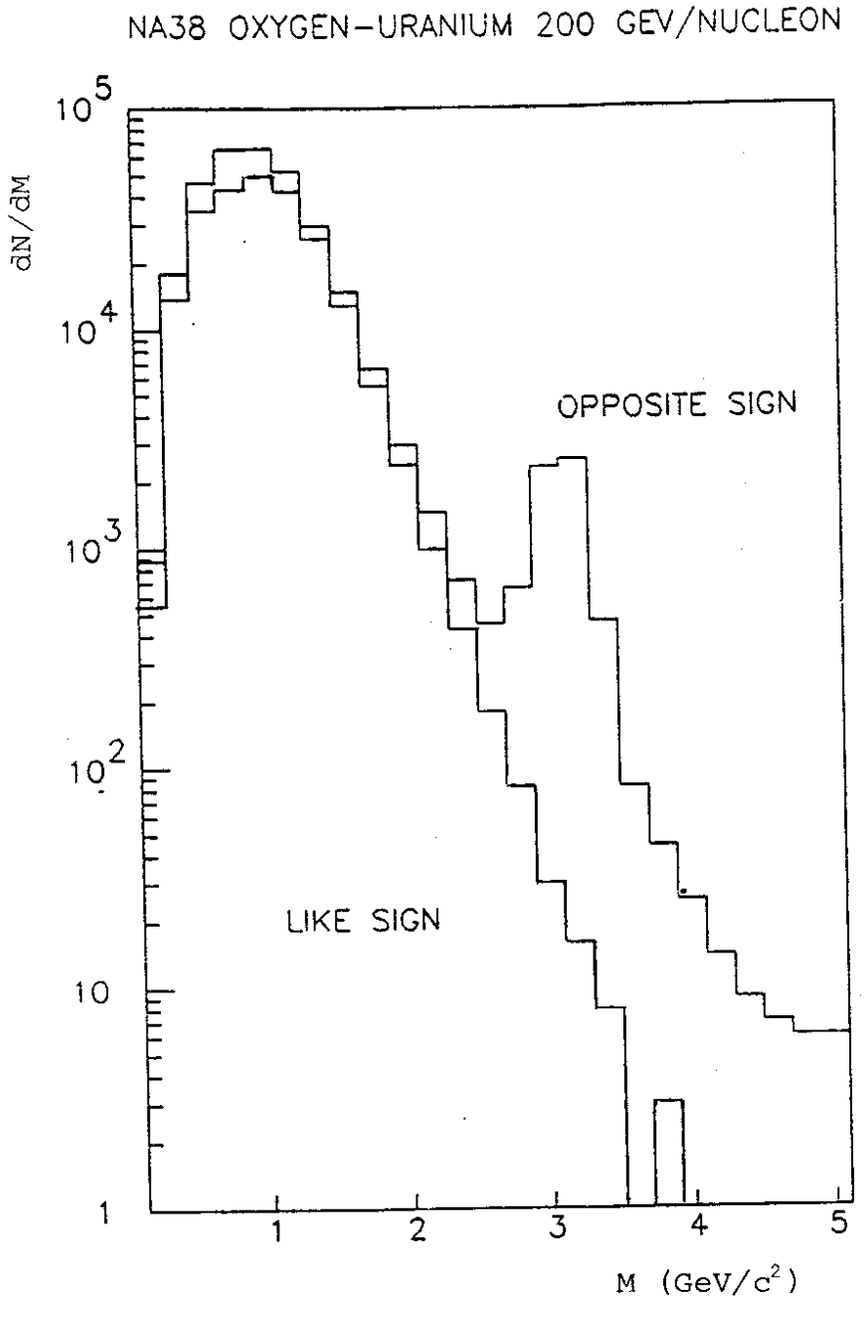
NA38 OXYGEN-URANIUM 200 GEV/NUCLEON
dN/dM
10^5
10^4
10^3
10^2
10
1
OPPOSITE SIGN
LIKE SIGN
1
2
3
4
5
M (GeV/c^2)

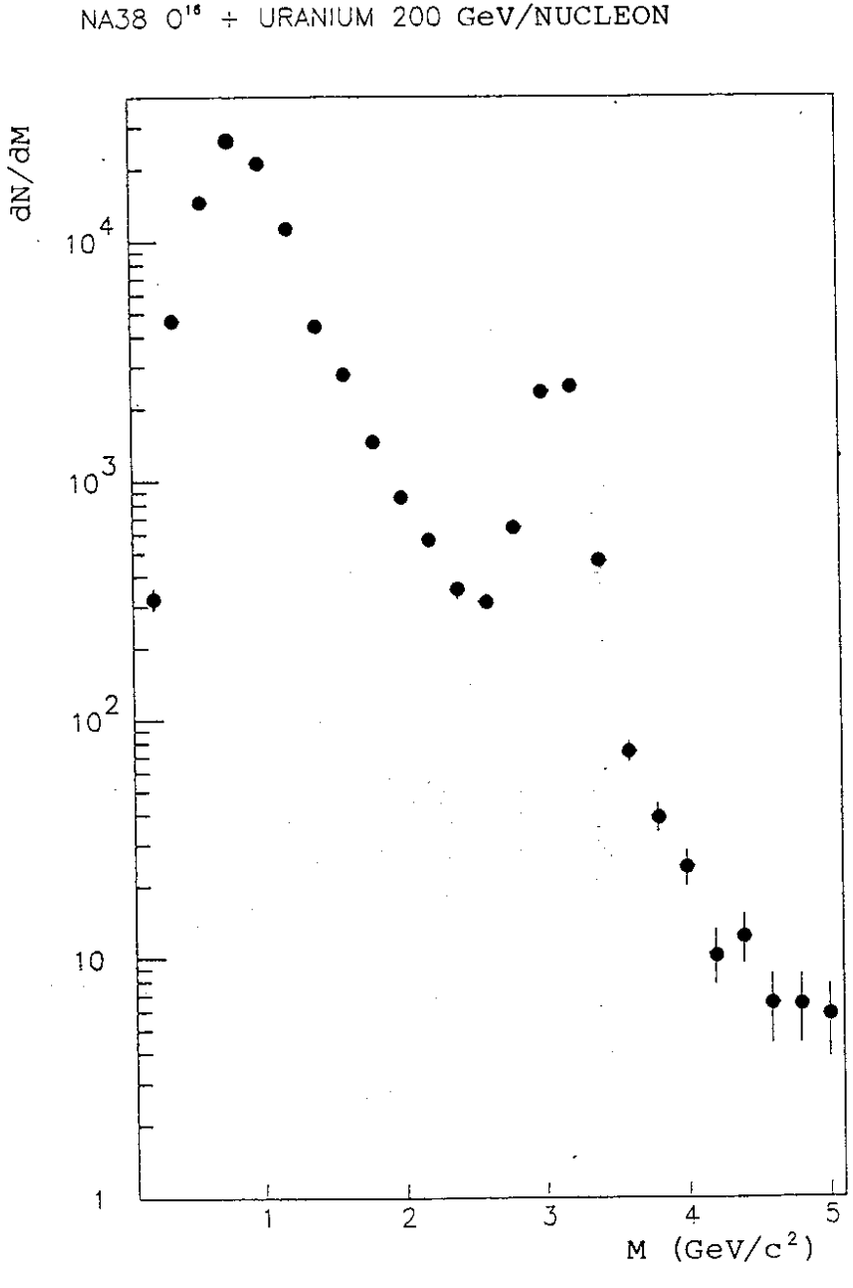
NA38 O^{16} + URANIUM 200 GeV/NUCLEON
dN/dM
10^4
10^3
10^2
10
1
1
2
3
4
5
M (GeV/c^2)

Fig.3

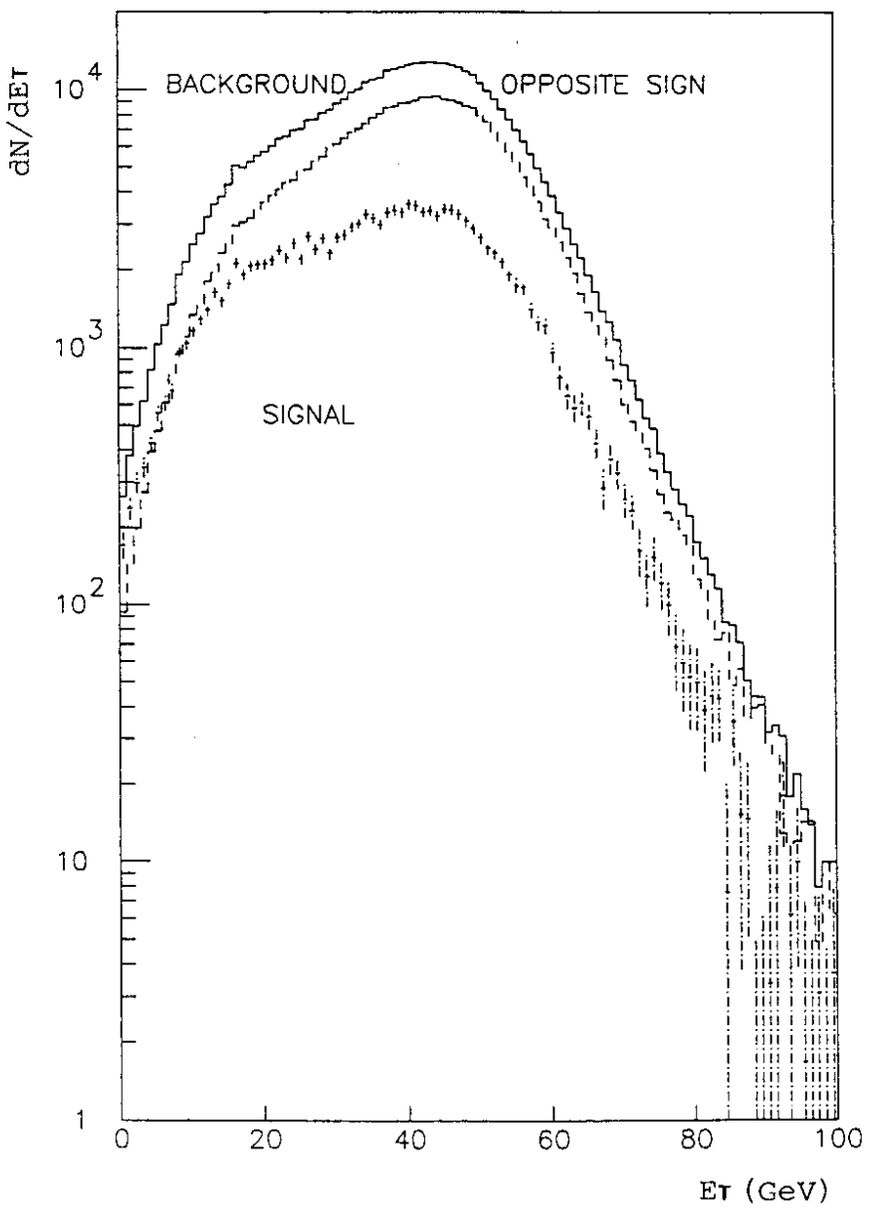
NA38 O16 + URANIUM 200 GeV/ NUCLEON
dN/dET
10^4
10^3
10^2
10
1
BACKGROUND
OPPOSITE SIGN
SIGNAL
0
20
40
60
80
100
ET (GeV)

Fig.4

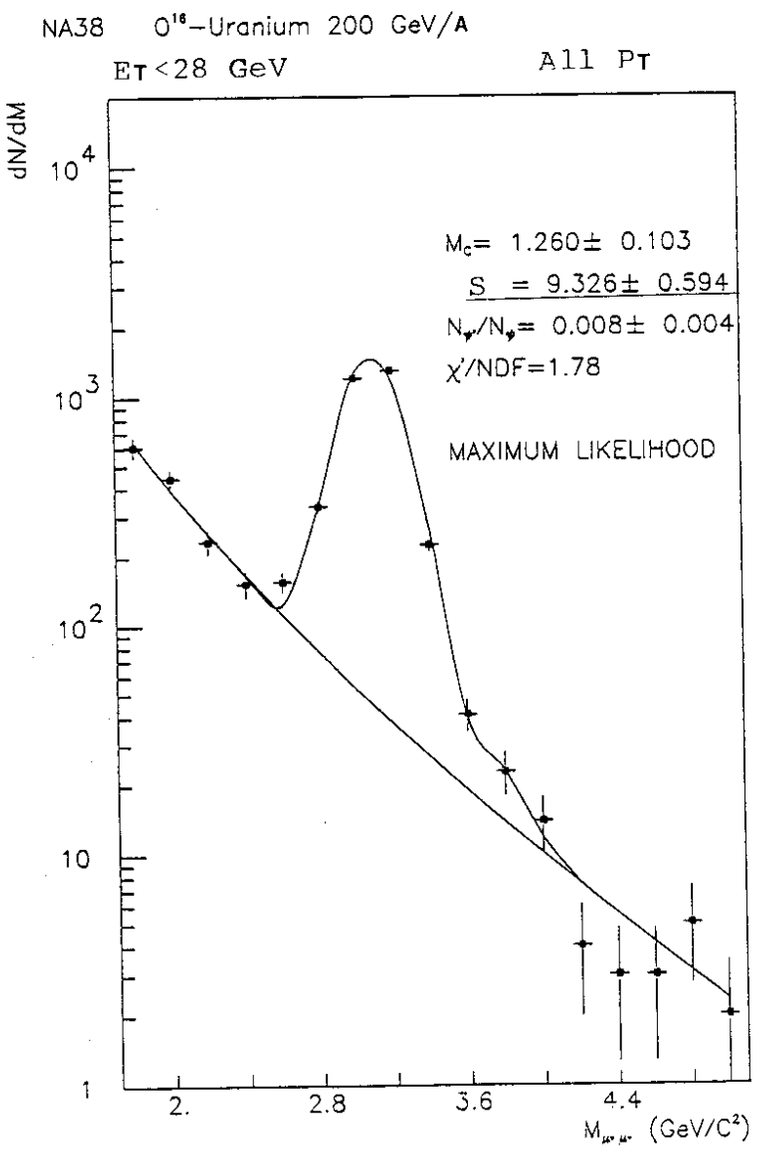
NA38 O16–Uranium 200 GeV/A
ET<28 GeV
All PT
dN/dM
10^4
10^3
10^2
10
1
Mc= 1.260± 0.103
S = 9.326± 0.594
Nψ'/Nψ= 0.008± 0.004
χ'/NDF=1.78
MAXIMUM LIKELIHOOD
2.
2.8
3.6
4.4
Mμ+μ- (GeV/C²)

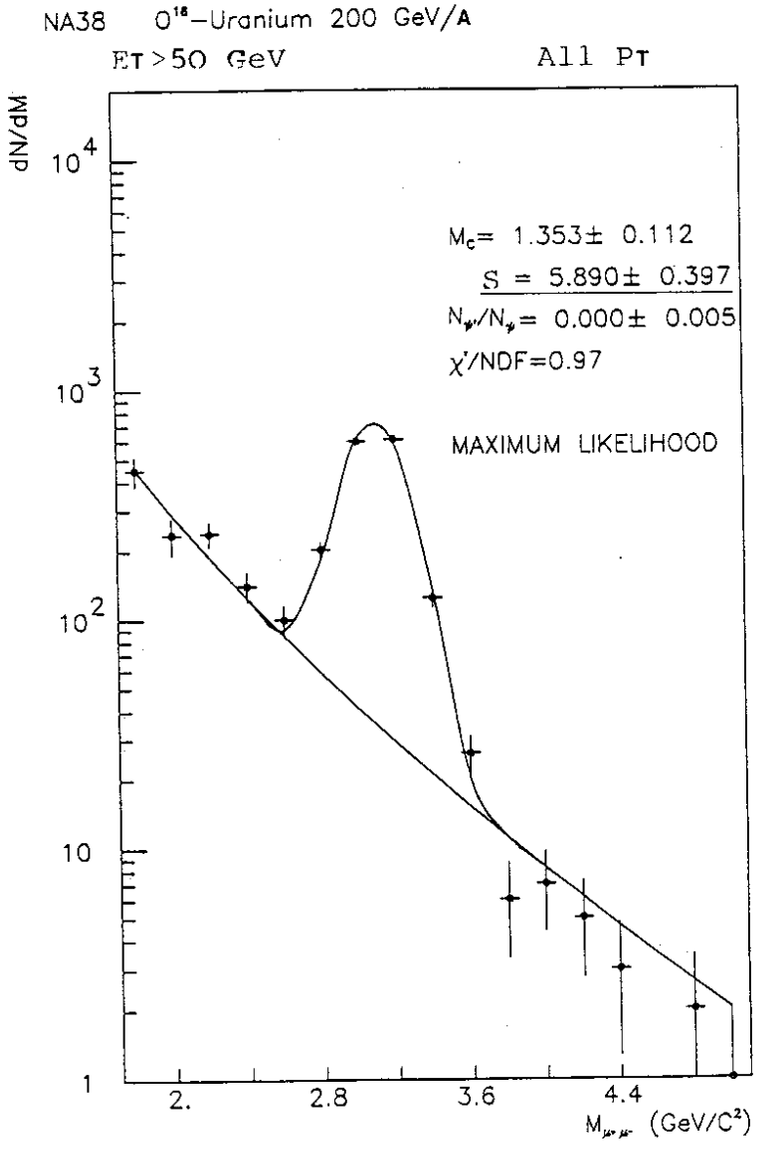
NA38 O16–Uranium 200 GeV/A
ET>50 GeV
All PT
dN/dM
10^4
10^3
10^2
10
1
Mc= 1.353± 0.112
S = 5.890± 0.397
Nψ'/Nψ= 0.000± 0.005
χ'/NDF=0.97
MAXIMUM LIKELIHOOD
2.
2.8
3.6
4.4
Mμ+μ- (GeV/C²)

Fig.5

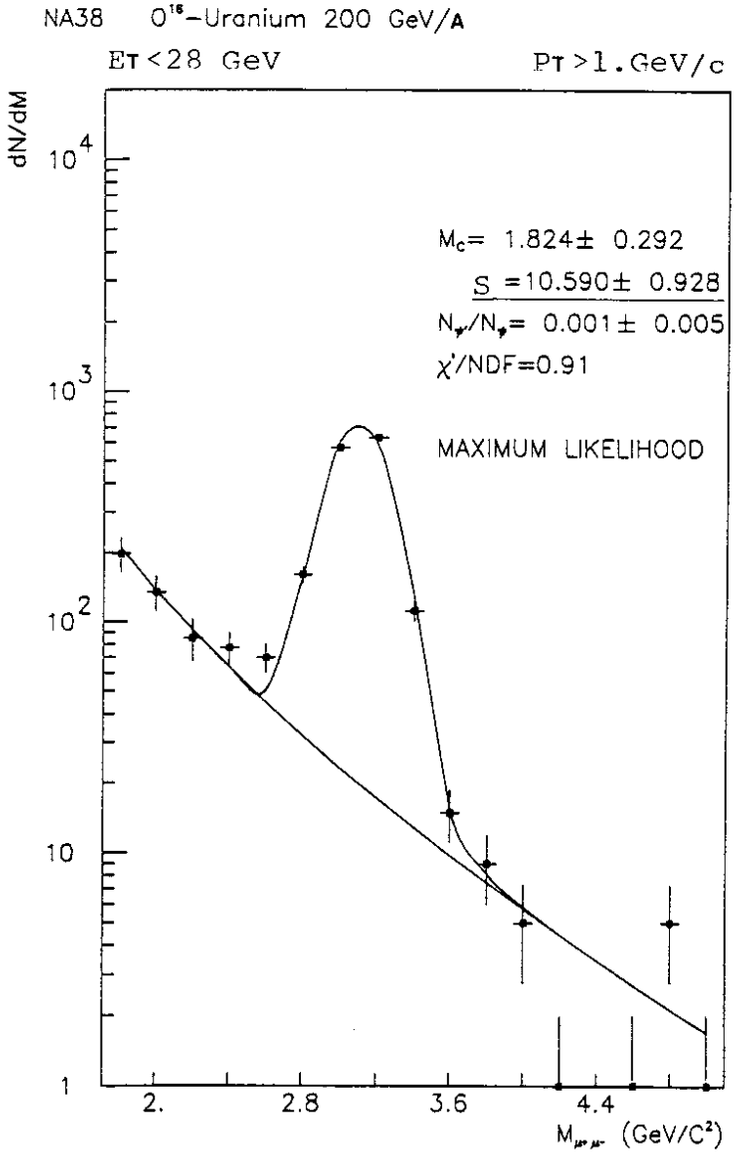
NA38 O16–Uranium 200 GeV/A
ET<28 GeV
PT>1.GeV/c
dN/dM
10^4
10^3
10^2
10
1
Mc= 1.824± 0.292
S =10.590± 0.928
Nψ'/Nψ= 0.001± 0.005
χ'/NDF=0.91
MAXIMUM LIKELIHOOD
2.
2.8
3.6
4.4
Mμ+μ- (GeV/C²)

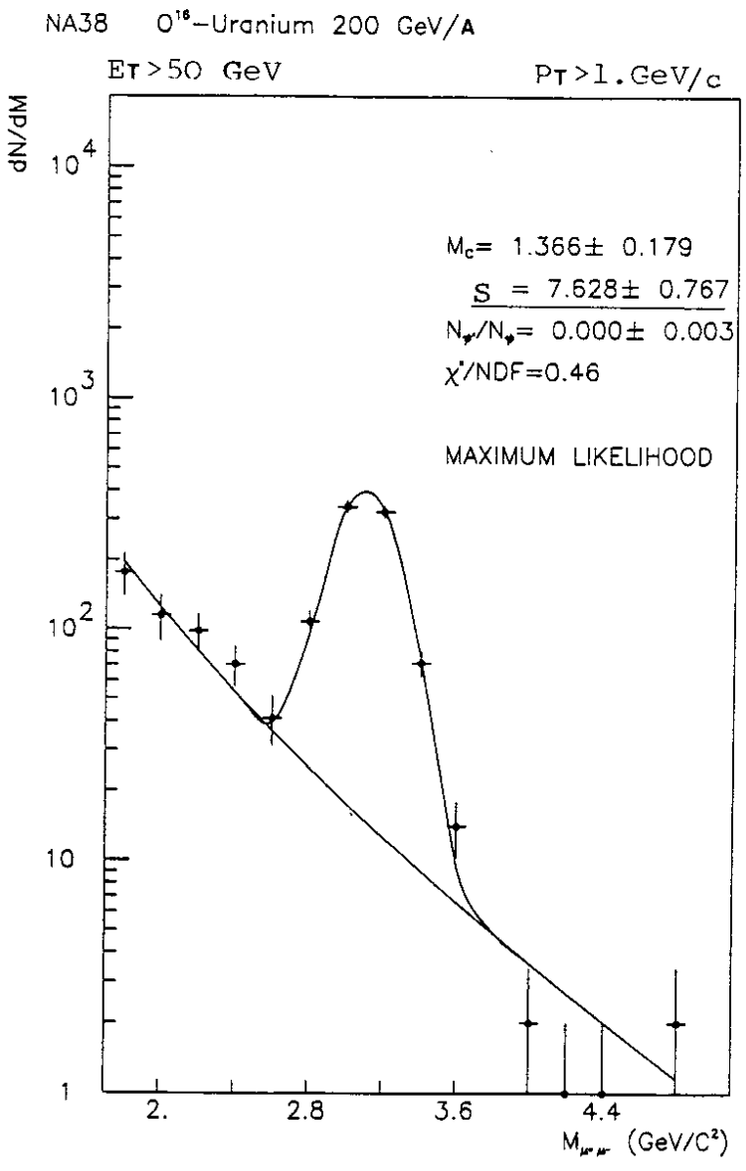
NA38 O16–Uranium 200 GeV/A
ET>50 GeV
PT>1.GeV/c
dN/dM
10^4
10^3
10^2
10
1
Mc= 1.366± 0.179
S = 7.628± 0.767
Nψ'/Nψ= 0.000± 0.003
χ'/NDF=0.46
MAXIMUM LIKELIHOOD
2.
2.8
3.6
4.4
Mμ+μ- (GeV/C²)

Fig.6

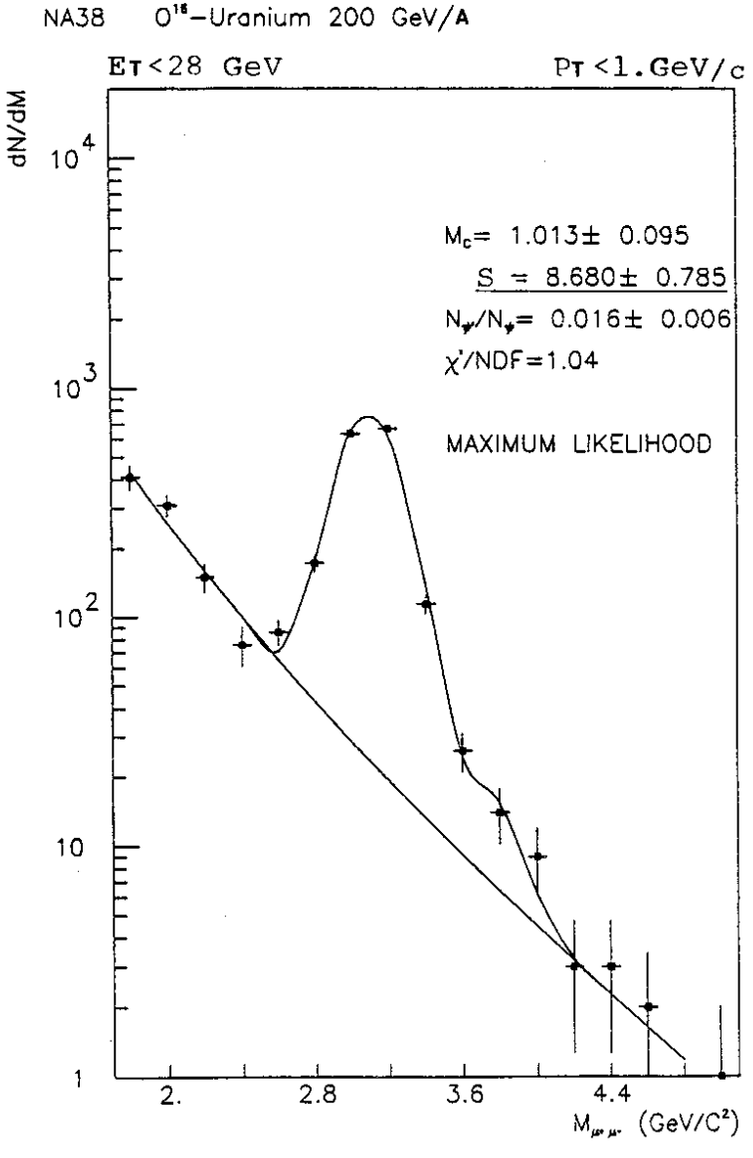
NA38 O16–Uranium 200 GeV/A
ET<28 GeV
PT<1.GeV/c
dN/dM
10^4
10^3
10^2
10
1
Mc= 1.013± 0.095
S = 8.680± 0.785
Nψ/Nφ= 0.016± 0.006
χ'/NDF=1.04
MAXIMUM LIKELIHOOD
2.
2.8
3.6
4.4
Mμ+μ- (GeV/C²)

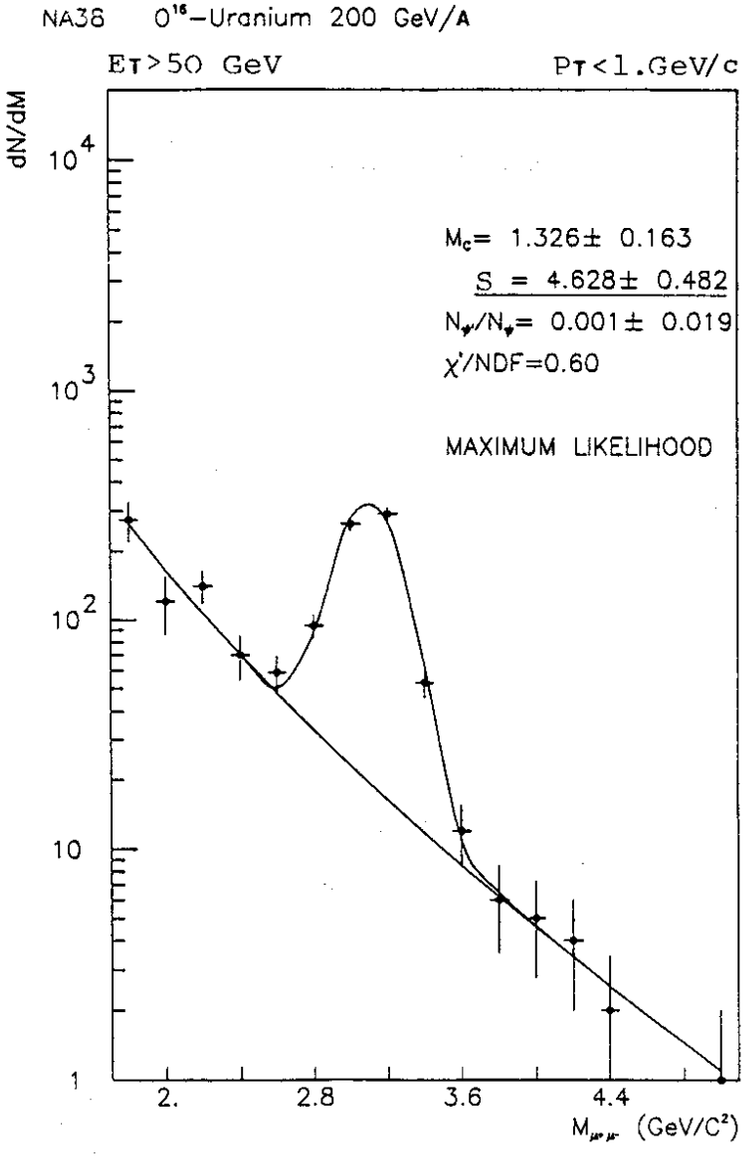
NA38 O16–Uranium 200 GeV/A
ET>50 GeV
PT<1.GeV/c
dN/dM
10^4
10^3
10^2
10
1
Mc= 1.326± 0.163
S = 4.628± 0.482
Nψ/Nφ= 0.001± 0.019
χ'/NDF=0.60
MAXIMUM LIKELIHOOD
2.
2.8
3.6
4.4
Mμ+μ- (GeV/C²)

Fig.7

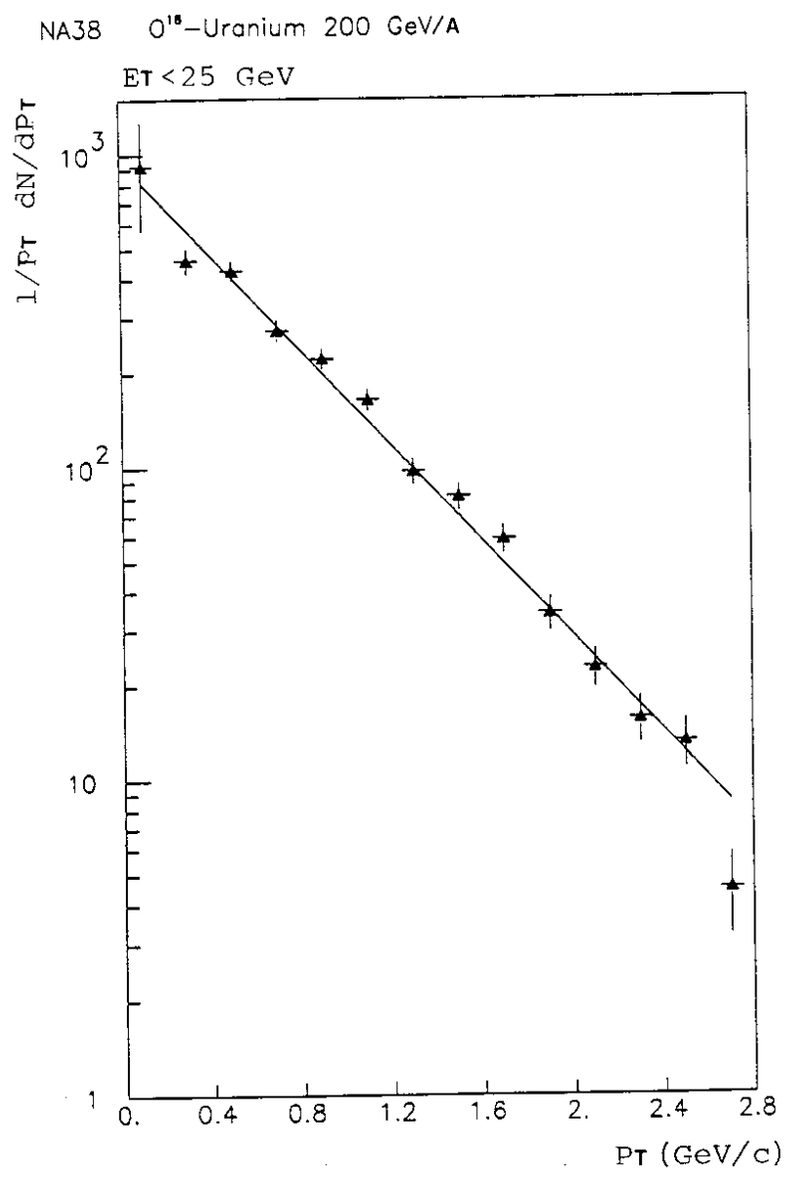
NA38 O16–Uranium 200 GeV/A
ET < 25 GeV
1/PT dN/dPT
10^3
10^2
10
1
0.
0.4
0.8
1.2
1.6
2.
2.4
2.8
PT (GeV/c)

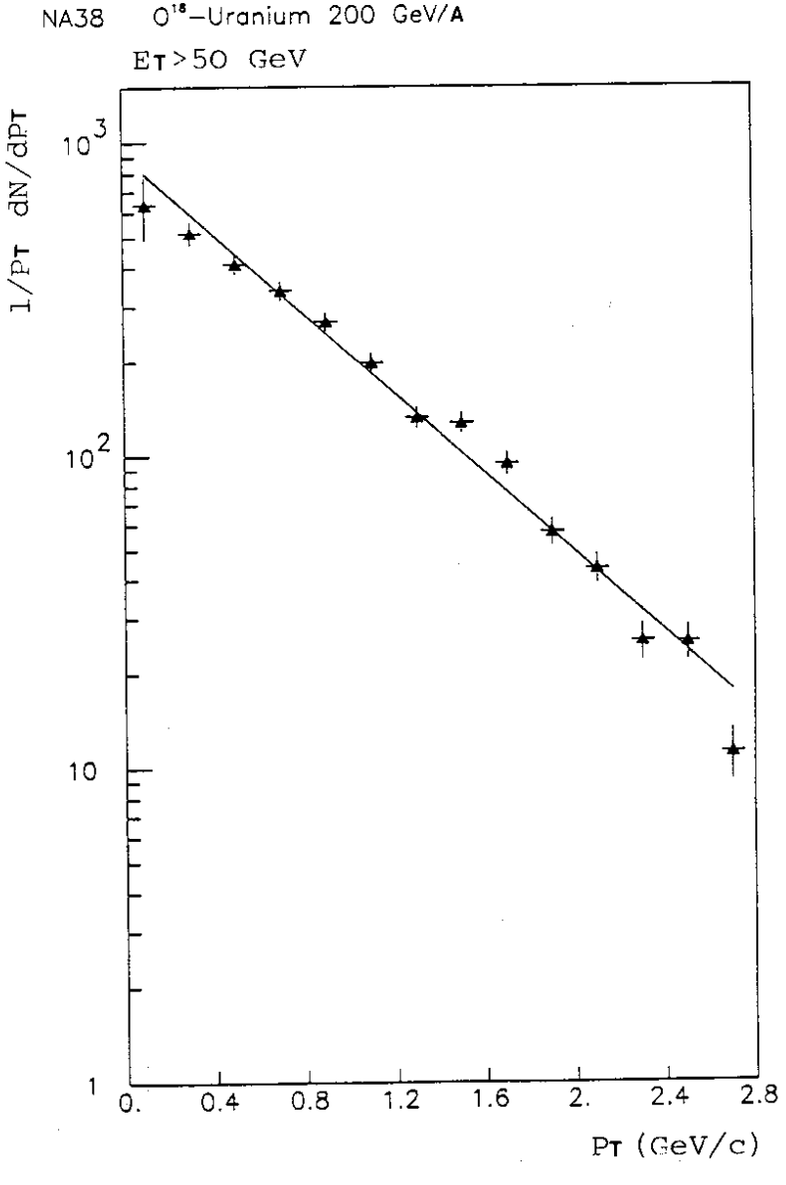
NA38 O16–Uranium 200 GeV/A
ET > 50 GeV
1/PT dN/dPT
10^3
10^2
10
1
0.
0.4
0.8
1.2
1.6
2.
2.4
2.8
PT (GeV/c)

Fig.8

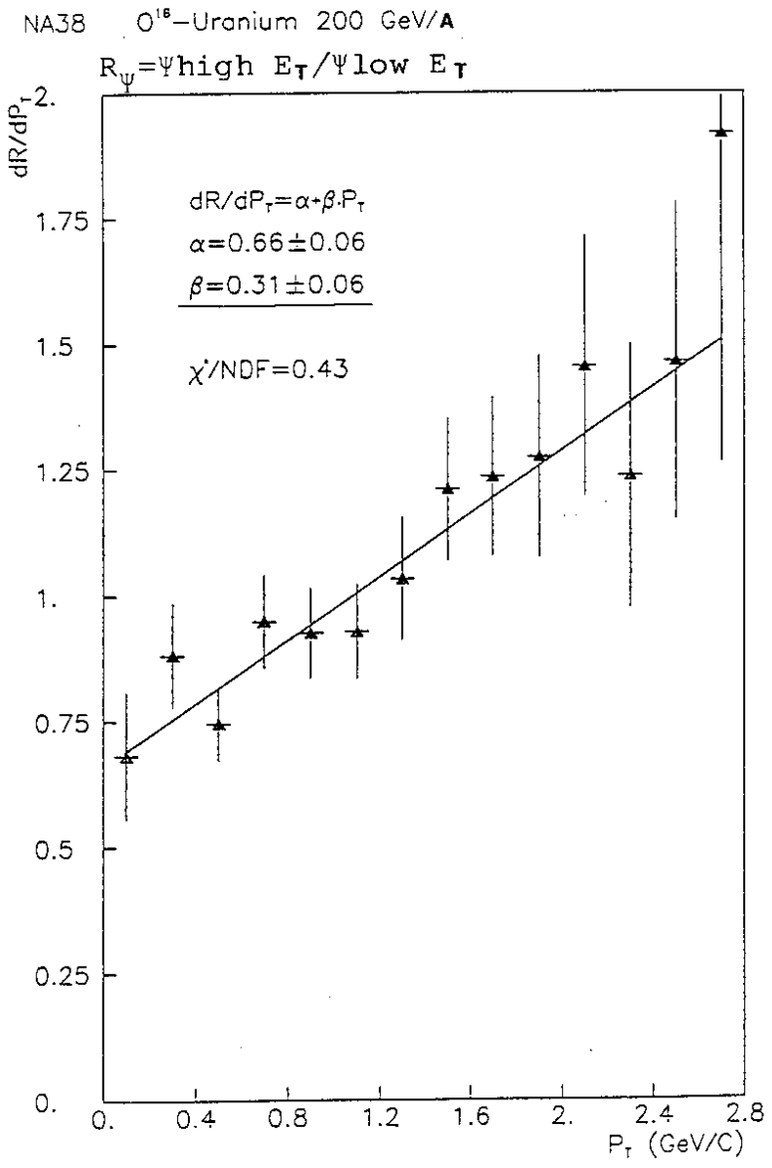
NA38 O16–Uranium 200 GeV/A
R_ψ=ψhigh E_T/ψlow E_T
dR/dP_T
dR/dP_T=α+β·P_T
α=0.66±0.06
β=0.31±0.06
χ²/NDF=0.43
2.
1.75
1.5
1.25
1.
0.75
0.5
0.25
0.
0.
0.4
0.8
1.2
1.6
2.
2.4
2.8
P_T (GeV/C)

Fig.9

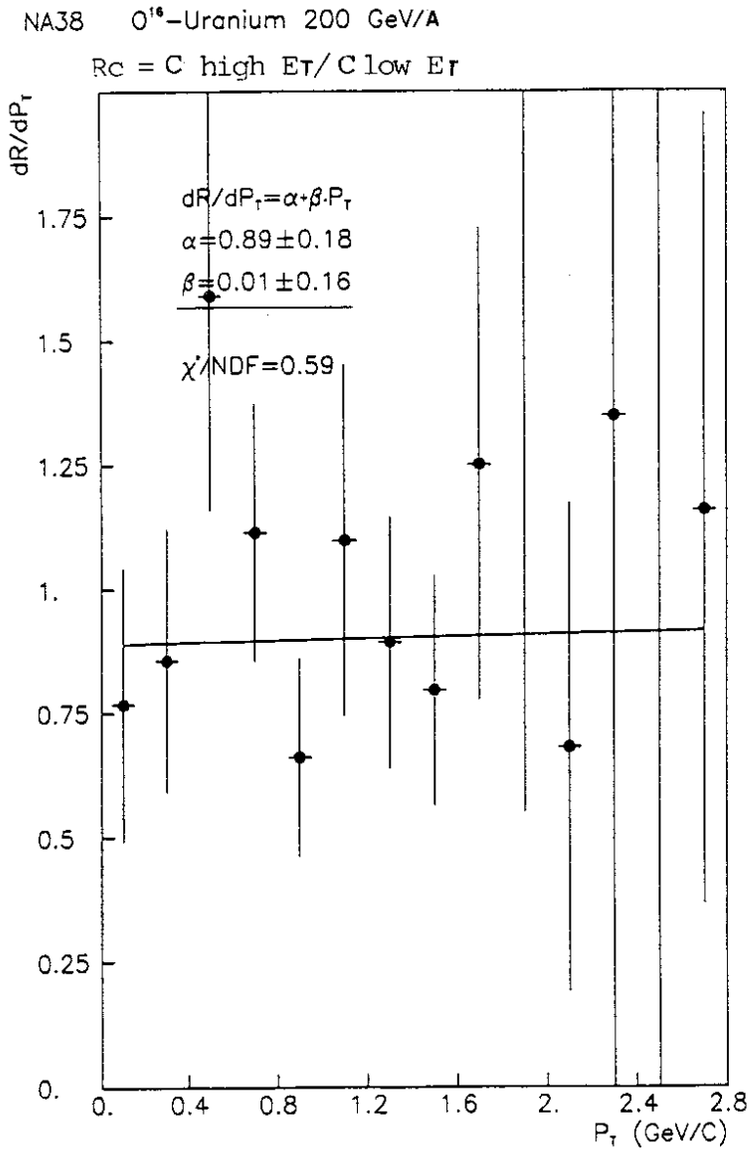
NA38 O16–Uranium 200 GeV/A
Rc = C high ET/ C low ET
dR/dPT
dR/dPT=α+β·PT
α=0.89±0.18
β=0.01±0.16
χ2/NDF=0.59
1.75
1.5
1.25
1.
0.75
0.5
0.25
0.
0.
0.4
0.8
1.2
1.6
2.
2.4
2.8
PT (GeV/C)

Fig.10

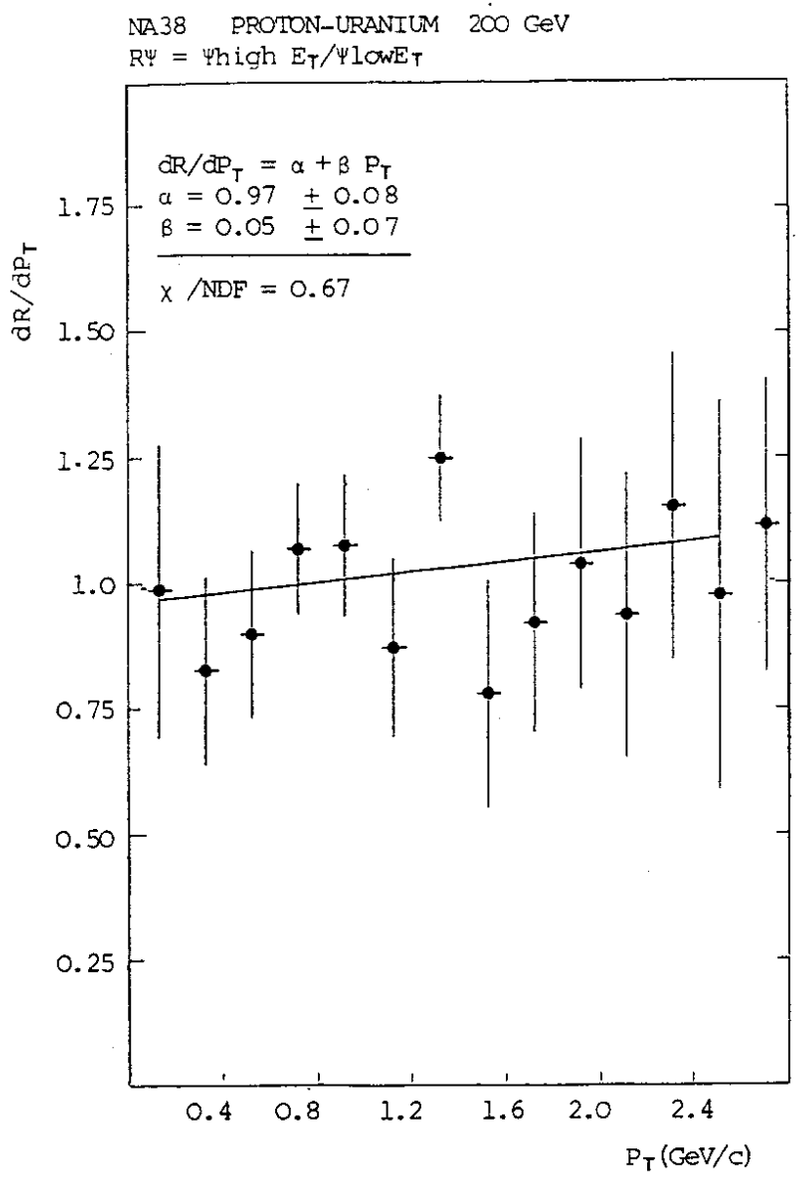
NA38 PROTON-URANIUM 200 GeV
RΨ = Ψhigh ET/ΨlowET
dR/dPT = α + β PT
α = 0.97 ± 0.08
β = 0.05 ± 0.07
χ /NDF = 0.67
dR/dPT
1.75
1.50
1.25
1.0
0.75
0.50
0.25
0.4
0.8
1.2
1.6
2.0
2.4
PT(GeV/c)

Fig.11